CHEMISTRY
A EUROPEAN JOURNAL

DOI: 10.1002/chem.200802682

Synthesis, Structure, and Highly Efficient Copper-Catalyzed Aziridination with a Tetraaza-Bispidine Ligand

Peter Comba,*[a] Christina Haaf,[a] Achim Lienke,[b] Amsaveni Muruganantham,[a] and Hubert Wadepohl[a]

Abstract: The distorted trigonal-bipyramidal Cu^{II} complex $[Cu(L^1)(NCCH_3)]^{2+}$ of the novel tetradentate bispidine-derived ligand L^1 with four tertiary amine donors (L^1 = 1,5-diphenyl-3-methyl-7-(1,4,6-trimethyl-1,4-diazacycloheptane-6-yl)diazabicyclo[3.3.1]-nonane-9-one) is a very efficient catalyst for the aziridination of olefins in the presence of a nitrene source. In agreement with the experimental data (in situ spectroscopy, product distribution, and its dependence on the geometry of the substrate and of the nitrene source), a theoretical analysis based on DFT calculations indicates that the active catalyst has the Cu center in its +II oxidation state, that electron transfer is not involved, and that the conversion of the olefin to an aziridine is a stepwise process involving a radical intermediate. The striking change of efficiency and reaction mechanism between classical copper–bispidine complexes and the novel L^1-based catalyst is primarily attributed to the structural variation, enforced by the ligand architecture.

Keywords: aziridination · copper · homogeneous catalysis · N ligands · reaction mechanisms

Introduction

The chemistry of three-membered ring heterocycles, especially that of the aziridines, has inspired organic chemistry for decades,[1–3] and the development of suitable methods for their synthesis has a long history.[4,5] Aziridines may be prepared by stoichiometric or catalytic reactions (see Scheme 1). In stoichiometric reactions, the efficiency strongly depends on the nitrogen source and the alkene precursor; the advantage is a good accessibility of chiral azirdines.[6,7] The transition-metal-catalyzed route is often used due to its efficiency, and many examples have been studied in detail.[1,3,5,8–13] Due to its high reactivity, PhINTs ([*N*-(*p*-toluenesulfonyl)imino]phenyliodinane) is generally used as the nitrene source, although others such as chloramine T have economic and ecological advantages.[4,5,8,14,15]

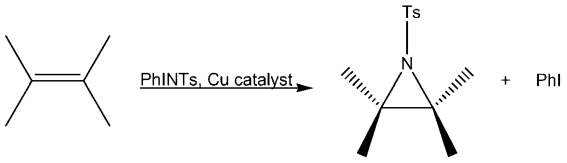

Scheme 1. Copper-catalyzed preparation of aziridines.

Various reaction mechanisms have been proposed for the transition-metal-catalyzed processes, and these include stepwise pathways with radical intermediates as well as concerted reactions, and nitrene complex intermediates with the metal ions in various oxidation states (e.g., for copper: Cu^{I}, Cu^{II}, Cu^{III}) have been suggested; mechanisms that do not include any electron-transfer steps at the metal center and Lewis acid based mechanisms with non-redox-active metal ions such as Zn^{2+} and Mg^{2+} have also been proposed.[5,8,16–20] We have characterized a series of $Cu^{II/I}$ couples with tetra- and pentadentate bispidine-based ligands (see L^2 for a tetradentate derivative),[21–28] and these were shown to be reasonably active aziridination catalysts.[19,29] We now describe the synthesis and characterization of the novel bispidine-type ligand L^1 and its Cu^{II} complex, as well as the highly efficient copper-catalyzed aziridination and a

[a] Prof. P. Comba, C. Haaf, Dr. A. Muruganantham, Prof. H. Wadepohl
Universität Heidelberg
Anorganisch-Chemisches Institut
INF 270, 69120 Heidelberg (Germany)
Fax: (+49) 6226-546617
E-mail: peter.comba@aci.uni-heidelberg.de

[b] Dr. A. Lienke
Unilever R&D Vlaardingen
Olivier van Noortlaan 120
3133AT Vlaardingen (The Netherlands)

Supporting information for this article is available on the WWW under http://dx.doi.org/10.1002/chem.200802682.

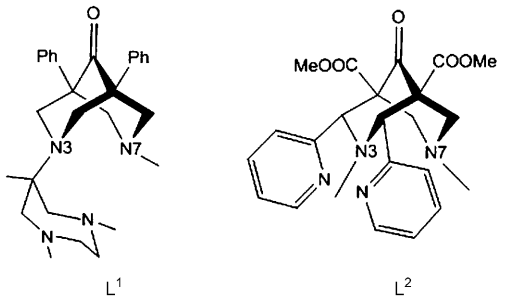

mechanistic analysis, based on spectroscopy, product analyses, and DFT calculations.

The transition-metal coordination chemistry of the traditional bispidines is rich in its structural variety and broad in its applications.[30] The majority of bispidine ligands reported so far has two or more aromatic nitrogen donor groups and enforces coordination geometries derived from *cis* octahedral with metal–donor distances and angular geometries around the metal center strictly enforced by the rigid adamantanoid bispidine backbone. Although complexes with specifically distorted *cis*-octahedral geometries, imposed by the first-generation bispidine ligands, for example, L^2, have produced exciting results,[30,31] specifically in the areas of ligand-enforced molecular geometries and the emerging properties,[32–35] and metal-ion-mediated oxygen activation,[36–40] we have designed a similarly rigid ligand system that may impose different coordination geometries to the metal center and offer a large variety of donor sets. We report here the first example of a second generation of bispidine ligands (L^1 versus L^2), in which the extra donors are exclusively due to substitution at the amine components of the Mannich reaction. This enabled us to prepare a ligand (L^1), which enforces a (distorted) trigonal-bipyramidal structure with tertiary amines as the only donor groups.

Results and Discussion

Synthesis and characterization of the copper(II) catalyst: The new bispidine ligand L^1 is based on the cyclic triamine 6-amino-1,4,6-trimethyl-1,4-diazacycloheptane, obtained in a simple two-step reaction from bulk chemicals.[41,42] In a two-step Mannich condensation, the cyclic triamine is transformed into the piperidone P^1 in acceptable yields (see Scheme 2). This general scheme gives access to a wide range of derivatives with differing donor sets and geometries. The tetraaza ligand L^1 is the first member of this novel family of ligands and is obtained in very good yield from P^1. A water-free sample of $[Cu^{II}(L^1)(NCCH_3)](BF_4)_2$ was obtained from the corresponding Cu^I complex, which reacted in situ with $AgBF_4$ to give the product.

Single crystals of $[Cu(L^1)(NCCH_3)](BF_4)_2{\cdot}CH_3CN$ were obtained from a solution of the complex in MeCN, and the structure was solved by X-ray diffraction. A plot of the molecular cation appears in Figure 1 and selected structural

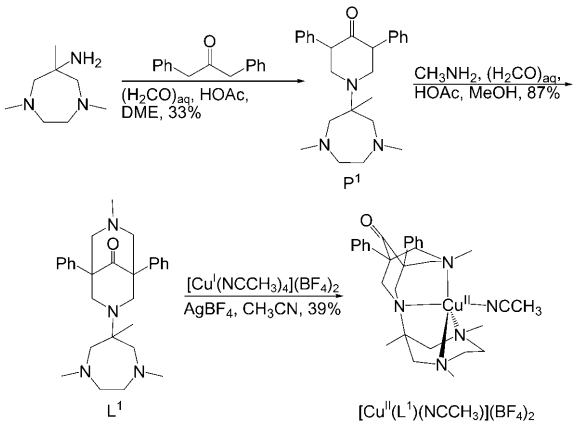

Scheme 2. Synthesis of $[Cu(L^1)(NCCH_3)]^{2+}$.

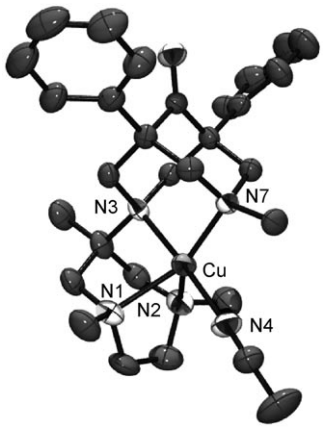

Figure 1. Molecular structure of $[Cu(L^1)(NCCH_3)]^{2+}$ (hydrogen atoms are omitted for clarity).

data are given in Table 1. The coordination geometry of the Cu^{II} center is distorted trigonal bipyramidal, with N3 of the bispidine ligand and the coordinated MeCN at axial positions. As expected from other bispidine complexes,[30,32] the bond lengths between Cu^{II} and the two tertiary amine nitrogen atoms of the bispidine backbone are approximately 2.0 Å. The bond lengths between the Cu^{II} center and the other equatorial amine nitrogen atoms (N1 and N2) are significantly longer. This may partially be due to the rather small angle of just under 77° between N1 and N2, enforced by the 5-membered chelate ring. As a result, the other two

Table 1. Selected structural parameters of $[Cu(L^1)(NCCH_3)](BF_4)_2{\cdot}CH_3CN$.

	Bond lengths [Å]		Valence angles [°]
Cu1–N7	2.032(3)	N3-Cu1-N4	176.75(15)
Cu1–N3	1.999(3)	N3-Cu1-N1	86.15(13)
Cu1–N1	2.169(4)	N3-Cu1-N2	83.85(14)
Cu1–N2	2.195(4)	N3-Cu1-N7	87.50(13)
Cu1–N4	1.969(4)	N1-Cu1-N2	76.56(14)
		N7-Cu1-N1	144.61(14)
		N7-Cu1-N2	137.14(14)

angles in the trigonal plane are much larger (137 and 145°); the angles between the axial and equatorial ligands are all around 90°. The bond from Cu^{II} to the axial MeCN coligand is 1.97 Å, thus in the expected range.

For a trigonal-bipyramidal geometry a $(d_{z^2})^1$ ground state is expected, and this should lead to the following spin Hamiltonian parameters: g factors $g_\perp > g_{||}$ and hyperfine structure constants $|A_\perp| \sim |A_{||}|$ (the A values are expected to be around 100 G, and the sign of $A_{||}$ is usually positive, whereas that of $A_\perp$ depends on the electronics and may vary).[43] The X-band EPR spectrum of $[Cu(L^1)(NCCH_3)]^{2+}$ has been measured and reveals a $d_{x^2-y^2}$ ground state ($g_{||}=2.21$, $g_\perp=2.08$, $A_{||}=170$ G, $A_\perp=156$ G; see the Supporting Information). This unconventional behavior is due to the relatively large distortion from trigonal-bipyramidal geometry. Specifically, the angular distortion within the "trigonal" plane (Cu^{II}, N1, N2, N7) leads to nondegenerate $d_{x^2-y^2}$ and d_{xy} orbitals and, in particular, to a destabilization of the $d_{x^2-y^2}$ orbital. This also follows from DFT calculations, which unambiguously show the $d_{x^2-y^2}$ orbital to be highest in energy of the d orbital manifold (see below and the Supporting Information).

Experimental mechanistic studies: $[Cu(L^1)(NCCH_3)]^{2+}$ is one of the most efficient catalysts for the aziridination of styrene with PhINTs.[17–19,29] Various solvents and catalyst/substrate/nitrene ratios were studied (see Table 2), and linear pseudo-first-order kinetic behavior for styrene concentrations up to 20 equivalents was observed (entries 5–7; a variation of the amount of PhINTs did not affect the aziridination reactivity). Nonpolar solvents are expected to favor radical reactions. However, changing the solvent from CH_3CN to noncoordinating solvents such as CH_3NO_2 or CH_2Cl_2/toluene, which were expected to accelerate the addition of PhINTs to the precatalyst, did not lead to higher reactivity. In contrast, smaller yields were observed in these experiments (entries 8–10). Therefore, it appears that in the aziridination reaction studied here, the solubility of the cationic catalyst and the poorly soluble PhINTs substrate are responsible for the observed reactivity trends. Catalytic aziridination experiments with trifluoromethanesulfonate instead of tetrafluoroborate as counterion did not show enhanced catalytic efficiency (entry 11).

Several observations suggested that the $\{Cu^{II}(L^1)\}^{2+}$-catalyzed process follows a novel pathway with a Cu^{II}–nitrene intermediate, which initiates a stepwise conversion of styrene to the corresponding aziridine, and therefore involves a radical intermediate and no change in the Cu^{II} oxidation state. The latter assumption is supported by UV/Vis spectra of $\{Cu^{II}(L^1)\}^{2+}$/PhINTs mixtures, in which no $\{Cu^{I}(L^1)\}^{+}$ was detected under conditions that allowed spectrophotometric trapping of Cu^I intermediates in other systems:[44] the spectrum in Figure 2 taken after the addition of PhINTs shows two bands in the UV region with increasing intensity but no significant change of the d–d transition in the visible region at $\lambda=630$ nm. This indicates that in the $\{Cu^{II}(L^1)\}^{2+}$/PhINTs system, there is no reduction of Cu^{II} to Cu^{I}. Attempts to trap and characterize a $\{Cu^{I}(L^1)\}^{+}$ complex failed because $\{Cu^{I}(L^1)\}^{+}$ readily disproportionates to $\{Cu^{II}(L^1)\}^{2+}$ and $\{Cu^0\}$. This is also evident from the irreversible electrochemical behavior of $\{Cu^{II}(L^1)\}^{2+}$ in MeCN ($E_{ir,Cu^I,Cu^{II}}=-377$ mV and $E_{ir,Cu^{II},Cu^{III}}=+1720$ mV, respectively, versus $Ag/AgNO_3$). The absence of any formation of $\{Cu^0\}$ (disproportionation of Cu^I, see above) is further support for our interpretation that $\{Cu^{II}(L^1)\}^{2+}$ is the active catalyst and does not change the oxidation state in the catalytic cycle.

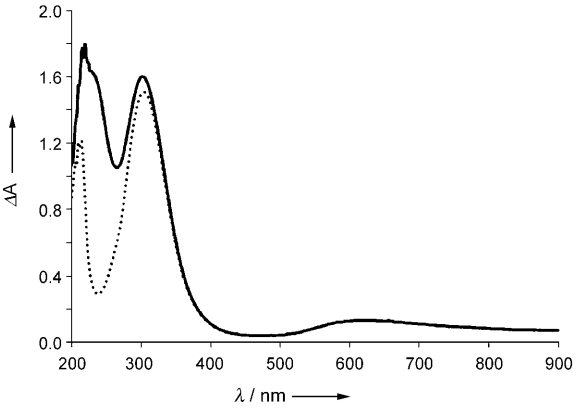

Figure 2. UV/Vis experiments: -----$=\{Cu^{II}(L^1)\}^{2+}$ (10^{-4} M in CH_3CN); ——$=\{Cu^{II}(L^1)\}^{2+}$+PhINTs (10^{-4} M in CH_3CN).

Table 2. Aziridination of styrene with PhINTs, catalyzed by $[Cu(L^1)(NCCH_3)]^{2+}$ in MeCN.[a]

Entry	Equiv styrene	Solvent [ml]	Catalyst [mol%]	t [min]	Yield [%]	TON[b]
1	22	CH_3CN (2)	5	5	88	18
2	22	CH_3CN (2)	0.5	40	85	168
3	22	CH_3CN (2)	0.25	200	85	339
4	1	CH_3CN (0.5)	1	27	70	70
5	20	CH_3CN (2)	1	11	92	92
6	10	CH_3CN (2)	1	28	91	91
7	1	CH_3CN (2)	1	47	87	87
8	22	CH_3NO_2 (2)	5	25	64	13
9	1	CH_3NO_2 (0.5)	2	30	17	17
10	1	CH_2Cl_2 (0.5)/toluene (2)	2	30	3	3
11[c]	1	CH_3CN (0.5)	1	30	40	40
12	22	CH_3CN (2)	0	420	0	0

[a] $[Cu(L^1)(NCCH_3)]^{2+}$ is the most efficient bispidine-derived aziridination catalyst reported so far and only slightly less efficient than recently reported Cu^{II} complexes.[18] The maximum efficiency observed with Cu complexes of bispidine ligands derived from L^2 are TON 270 in 24 h (5 mol% cat., 46% yield, 24 h).[19,29] [b] TON = n(product)/n(catalyst). [c] Experiments carried out with $[Cu(L^1)(NCCH_3)](O_3SCF_3)_2$.

The $[Cu(L^1)(NCCH_3)]^{2+}$-catalyzed conversion of *cis*-β-methylstyrene with PhINTs produces both *cis*- and *trans*-aziridine products (19% *trans*, see Table 3), which suggests that the aziridination is a stepwise process with a radical intermediate of significant life time.[5] Due to this radical, there is stereochemical scrambling at the former double bond as shown by the value of 62% for the diastereomeric

Table 3. Stereoselective aziridination of *cis*-β-methylstyrene with PhINTs, catalyzed by $[Cu(L^1)(NCCH_3)]^{2+}$ in MeCN.

Nitrene source	*cis*/*trans* ratio	*de*[a] [%]	*t* [min]	Yield [%]
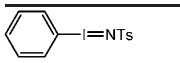	81:19	62	85	68
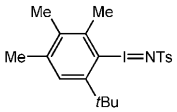	84:16	68	120	100

[a] *de* = diastereomeric excess.

excess (*de*). To confirm the proposed radical-based mechanism, a sterically more demanding PhINTs derivative was also used as a nitrene source. PhI is assumed to be fully dissociated from the nitrene source in the radical intermediate (see also "Computational studies" below) but covalently bound in a Lewis acid process.[5] Bulky substituents on the PhI group are therefore expected to change the *cis*/*trans* ratio in the aziridination product of *cis*-β-methylstyrene in the case of a Lewis acid based process but not in a radical mechanism. The fact that there is no significant change of the product ratio as a function of steric bulk (62 vs. 68% *de*, see Table 3) indicates that the $\{Cu^{II}(L^1)\}$-catalyzed aziridination with PhINTs derivatives follows a radical-based mechanism.

Computational studies: DFT calculations were used to confirm the mechanistic conclusions derived from the experiments and to understand the fundamental reasons for the change of mechanism between the complexes discussed here and other Cu-based aziridination catalyst systems.[19,20,29,45,46] Based on published experimental and computational observations, Scheme 3 was adopted for the DFT calculations. In the initial step, $[Cu(L^1)(NCCH_3)]^{2+}$ reacts with PhINTs to form a $\{Cu^{II}(L^1)\cdots PhINTs\}$ precursor. Optimization of this

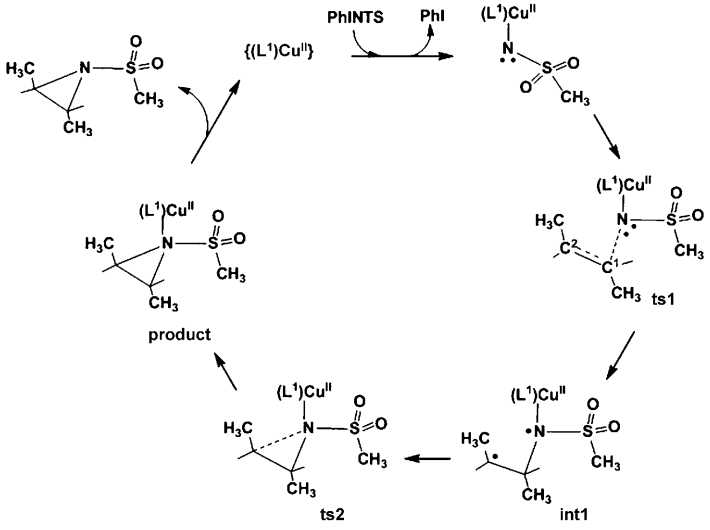

Scheme 3. Proposed mechanistic scheme for the aziridination reaction due to $\{Cu^{II}(L^1)\}^{2+}$.

adduct reveals that PhI is immediately dissociated to form a Cu^{II} nitrene species in a fast and facile reaction. This is in contrast to observations in similar computational studies with other bispidine-based aziridination catalysts[19,29] but is consistent with the data presented in Table 3.

Due to the rigidity and steric demand of the bispidine ligand system and the enforced trigonal-bipyramidal geometry, but in contrast to similar reactions with other bispidine-derived catalyst systems,[19,29] the nitrene only acts as a monodentate ligand. The catalytically active Cu^{II} nitrene species has two unpaired electrons on the nitrene N and one on the Cu^{II} center, and a quartet as well as a doublet spin state is possible. The doublet is the ground state (direct exchange between Cu ($d_{x^2-y^2}$) and $N_{nitrene}$ orbitals), with the quartet state at 35.7 kJ mol^{-1}. The doublet ground state has a distorted trigonal-bipyramidal structure with the $N_{nitrene}$ *trans* to N3 on the pseudo-trigonal axis (see Figure 3), and

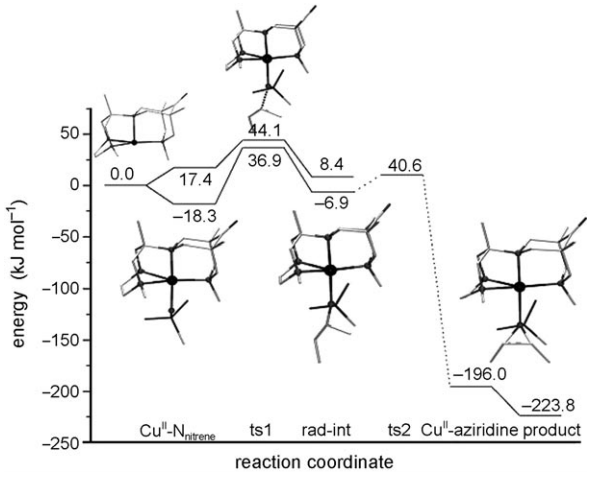

Figure 3. Potential-energy diagram of the aziridination reaction with optimized structures of the relevant species (rad-int = radical intermediate): doublet ($S = {}^1/_2$, lower energy), quartet ($S = {}^3/_2$, higher energy). The optimized structures shown are those of the $S = {}^1/_2$ pathway, those on the $S = {}^3/_2$ reaction are similar (see Table 3) and not shown for clarity.

the distribution of the spin density as expected for a doublet state (Cu: −0.255, $N_{nitrene}$: 1.329; the spin densities on the Cu^{II} center and all nitrogen atoms in the coordination sphere are given in Table 5; Table 4 reports selected structural parameters of the computed structures). The excess spin density on $N_{nitrene}$ facilitates the oxidation of the olefin. The spin on the Cu^{II} center is located in the $d_{x^2-y^2}$ orbital, as observed in the EPR spectrum of the $[Cu(L^1)(NCCH_3)]^{2+}$ precursor complex (see above and the Supporting Information), with the lobes of the orbital directed towards N2, N3, N7, and $N_{nitrene}$, in which spin delocalization is dominating. The now axial N1–Cu bond is significantly elongated (2.409 Å) and therefore gains spin density mainly through spin polarization (see Tables 4 and 5). The drastic reduction of spin density on $N_{nitrene}$ in the doublet as compared to the quartet state is due to strong spin delocalization, that is, in

Table 4. Selected B3LYP-computed structural parameters of the reactants, transition states (ts), intermediates (int), and products in the aziridination of alkenes, catalyzed by $[Cu(L^1)(NCCH_3)]^{2+}$ (see Scheme 3).

	Cu^{II}–complex	$^2Cu^{II}$–nitrene	$^4Cu^{II}$–nitrene	^{2}ts1	^{4}ts1	^{2}int1	^{4}int1	Cu^{II}–aziridine
E [kJ mol^{-1}]	0.0	−18.3	17.4	36.9	44.1	−6.9	8.4	−196.0
bond lengths [Å]								
Cu–N7	2.004	2.096	2.112	2.148	2.154	2.156	2.162	2.201
Cu–N3	2.033	2.006	2.069	2.091	2.090	2.096	2.101	2.103
Cu–N1	2.182	2.409	2.470	2.424	2.434	2.514	2.462	2.179
Cu–N2	2.144	2.166	2.120	2.229	2.221	2.168	2.211	2.627
Cu–$N_{nitrene}$	–	1.948	2.032	2.202	2.205	2.242	2.224	2.306
Cu–O	–	3.316	3.768	2.976	3.013	3.076	3.007	2.706
$N_{nitrene}$–C1	–	–	–	1.994	2.039	1.496	1.481	1.557
$N_{nitrene}$–C2	–	–	–	2.777	2.805	2.507	2.504	1.545
valence angles [°]								
N7-Cu-$N_{nitrene}$	–	92.2	94.9	95.9	95.8	96.8	97.5	95.6
N3-Cu-$N_{nitrene}$	–	173.4	170.6	177.9	178.3	174.6	176.8	168.3
N1-Cu-$N_{nitrene}$	–	99.3	90.5	97.4	96.9	96.1	97.1	99.8
N2-Cu-$N_{nitrene}$	–	88.3	95.7	94.5	95.7	95.1	94.2	93.2
Cu-$N_{nitrene}$-S	–	114.6	136.7	104.7	106.1	107.2	105.9	100.3
$N_{nitrene}$-C1-C2	–	–	–	107.7	107.0	113.3	113.5	60.8
N7-Cu-N1	137.9	141.6	137.0	143.1	142.8	137.1	139.1	152.2
N7-Cu-N2	143.4	143.0	147.1	139.2	139.3	145.4	142.7	131.1

Table 5. Calculated spin densities of various species along the potential-energy surface for the aziridination of alkenes, catalyzed by $[Cu(L^1)(NCCH_3)]^{2+}$ (see Scheme 3).

	Cu^{II}–complex	$^2Cu^{II}$–nitrene	$^4Cu^{II}$–nitrene	^{2}ts1	^{4}ts1	^{2}int1	^{4}int1	Cu^{II}–aziridine
Cu	0.549	−0.255	0.421	−0.513	0.504	−0.501	0.485	0.531
N7	0.099	−0.026	0.142	−0.105	0.119	−0.106	0.123	0.109
N3	0.277	−0.101	0.189	−0.177	0.189	−0.192	0.196	0.175
N1	−0.002	0.080	−0.148	−0.008	0.048	−0.001	0.038	0.098
N2	0.015	−0.060	0.116	−0.047	0.050	−0.062	0.062	0.003
$N_{nitrene}$	–	1.329	1.726	1.195	1.273	1.008	1.028	0.034
O1	–	0.030	0.156	0.059	0.088	0.033	0.039	0.003
O2	–	0.029	0.057	0.025	0.034	−0.003	0.002	−0.000
C1	–	–	–	−0.003	0.029	−0.085	−0.078	0.001
C2	–	–	–	0.637	0.645	0.893	0.945	0.001
S	–	−0.049	−0.053	−0.045	−0.043	−0.010	−0.005	−0.001

the doublet state the negative spin density on the copper center is transferred to $N_{nitrene}$.

Once the Cu^{II}–nitrene species is formed and reacts with an alkene, the conversion to the aziridine product may occur either by a concerted or a stepwise process. All attempts to optimize a transition state for a concerted reaction lead to the intermediate of the stepwise pathway, and a relaxed coordinate scan had an energy barrier much higher than that of the stepwise reaction (138 vs. 55 kJ mol^{-1}; the computed bond lengths of the species on the potential-energy surface are given in Table 4). The formation of the doublet nitrene precursor is exothermic by −18.3 kJ mol^{-1} but the quartet nitrene precursor is endothermic by +17.4 kJ mol^{-1}. Starting with the nitrene precursor, the first energy barrier (transition state 1, ts1) is 55.2 kJ mol^{-1} on the doublet and 26.7 kJ mol^{-1} on the quartet spin surface. This leads to the radical intermediate, with the doublet radical being endothermic by 11.4 kJ mol^{-1}, relative to the nitrene precursor; formation of the quartet radical is exothermic by −9.0 kJ mol^{-1}.

The stepwise pathway is consistent with the observed *cis*/*trans* product mixture. Calculations to estimate the C–C rotation barrier of the doublet radical intermediate were performed by a relaxed coordinate scan and gave an energy barrier of approximately 14 kJ mol^{-1}, which supports a possible *cis*/*trans* conversion during the ring-closure step (the energy barrier for the product-formation step is approximately 48 kJ mol^{-1}, see below). To examine the effect of different substrates, we have also calculated the rotational barriers for other radical intermediates, such as those derived from other common substrates, that is, but-2-ene and pent-2-ene in addition to *cis*-β-methylstyrene. The results suggest that the substitution pattern has only a small influence on the rotation-barrier height at the doublet radical intermediate stage (differences of the maxima are less than 5 kJ mol^{-1}, see the Supporting Information, i.e., the rotational barrier is always significantly lower than the barrier for product formation). We have not been able to locate a true transition state for the product-formation step (decay of the radical intermediate to the aziridination product but a relaxed coordinate scan reveals that the barrier height on the doublet surface is approximately 40 kJ mol^{-1}. The final product with a doublet ground state is exothermic by −196.0 kJ mol^{-1} from the reactant and by −177.7 kJ mol^{-1} from the nitrene precursor. The cleavage of the Cu–aziridine complex to regenerate the Cu^{I} catalyst is an exothermic process by −27.8 kJ mol^{-1}.

The structural parameters presented in Table 4 and the spin densities in Table 5 show the development of the course of the reaction along the potential-energy surface. In ts1, when the alkene approaches the nitrene complex, the Cu–$N_{nitrene}$ distance is significantly elongated from 1.948 to 2.202 Å, and therefore is weakening the Cu–$N_{nitrene}$ bond. Also, the spin density on the $N_{nitrene}$ atom decreases significantly in ts1 (1.329 to 1.195 Å), as expected when a new bond is formed. The transfer of spin density from $N_{nitrene}$ to

the newly forming nitrogen–carbon bonds occurs as expected through spin polarization. Moreover, the spin density on the carbon atoms of the alkene in ts1 is significant and suggests that the alkene already has radical character in the transition state. In the successive steps the radical intermediate has a further elongated $Cu–N_{nitrene}$ bond and a decreased spin density. These trends continue until the $Cu–N_{nitrene}$ bond stretches to 2.31 Å with spin densities close to zero in the Cu^{II}–aziridination product. At the very long distance of 2.31 Å the $Cu–N_{nitrene}$ bond is susceptible to cleavage and results in the release of the aziridination product and regeneration of the catalyst.

Conclusion

With the novel tetradentate bispidine ligand system L^1, we have been able to enforce a distorted trigonal-bipyramidal Cu^{II} coordination geometry, and this produces a very efficient aziridination catalyst that is shown to follow a mechanistic scheme that has not been observed before. The PhINTs moiety couples under cleavage of PhI with the Cu^{II} precatalyst. This leads to a relatively low-energy Cu^{II}–nitrene complex that produces a radical intermediate with long enough lifetime to allow for structural rearrangement. Experimentally, the fact that Cu^{II} is not reduced along the catalytic cycle, is supported by electronic spectroscopy and electrochemistry, and a radical intermediate with significant lifetime emerges from the stereochemical scrambling with *cis*-β-methylstyrene as substrate. The computed energetics (see Figure 3) suggest that the entire aziridination reaction occurs on the doublet spin surface. However, as the gap is small at the first transition state, there might be some involvement of the quartet state in the early stages of the reaction. As expected from the experimental observations, the reaction is thermodynamically favorable and the energy barriers are small compared with other aziridination reactions.[19,20,29,45,46] The important differences between this and other Cu-catalyzed aziridination reactions are 1) the ligand-enforced structure of the catalytically active Cu–nitrene complex with an unusual electronic ground state; 2) energetically unfavorable electron transfer (i.e., the reduction of the Cu^{II}–nitrene to a Cu^{I}–nitrene precursor does not occur; the computed energy difference of 13.9 kJ mol^{-1} indicates that, in contrast to other systems, this is an endothermic process, as observed experimentally); 3) lower energy barriers and higher thermodynamic stability of the products, driving the reaction faster along the potential-energy surface; 4) facile regeneration of the active catalyst.

Experimental Section

Materials and measurements: Chemicals and absolute solvents (ABCR, Aldrich, Fluka) were used without further purification if not otherwise noted. Styrene was distilled and stored under argon at −33 °C. NMR spectra were recorded at 200.13 (^{1}H) and 50.33 MHz (^{13}C) on Bruker AS-200 or Bruker DRX-200 instruments, respectively, with deuterated solvents as reference. IR measurements were performed with a Perkin–Elmer 16 PC FTIR instrument as KBr pellets. Mass spectra were recorded on a JEOL JMS-700 or a Finnigan TSQ 700/Bruker ApexQe hybrid 9.4 FT-ICR instrument; nibeol = 4-nitrobenzyl alcohol. Electronic spectra were obtained from a Tidas II J&M spectrophotometer. EPR spectra were measured on a Bruker ELEXSYS-E-500 instrument at 125 K, spin Hamiltonian parameters were obtained by simulation of the spectra with XSophe.[47,48] For electrochemical measurements, a BAS-100B workstation with a three-electrode setup, consisting of a glassy carbon working electrode, a Pt-wire auxiliary electrode, and $Ag/AgNO_3$ reference electrode (0.01 M Ag^+, 0.1 M $(Bu_4N)(PF_6)$ in CH_3CN, dry, degassed, under Ar), was used; the potential of the Fc^+/Fc couple had a value of 91 mV in CH_3CN . Elemental analyses were obtained from the analytical laboratories of the chemical institutes at the University of Heidelberg, using a Vario EL instrument of Elementar.

Caution: Although no difficulties were observed with the perchlorate salts of the complexes described here, these are potentially explosive and should be handled with extreme care. Heating, especially when dry, must be avoided.

1-(1,4,6-Trimethyl-1,4-diazacycloheptane-6-yl)-3,5-diphenylpiperidine-4-one (P^1): 1,4,6-trimethyl-6-amino-1,4-diazacycloheptane[41,49] (6.0 g, 38.1 mmol) was dissolved in 1,2-dimethoxyethane (DME; 20 mL). At 0 °C glacial acetic acid (7.5 mL) and formaldehyde solution (6.4 g, 79.1 mmol) were added, followed by 1,3-diphenylpropane-3-one (8.0 g, 38.1 mmol) at RT. The reaction mixture was stirred at 90 °C for 6 h. After cooling to RT all solvents were removed in vacuo and the resulting red oil was suspended in diethyl ether (500 mL). 70 % $HClO_4$ was added slowly with rigorous stirring to precipitate the piperidone perchlorate. The precipitate was washed with 1:1 EtOH/H_2O and crystallized from CH_3CN/diethyl ether (1:1) to yield the monoperchlorate salt of the piperidone. This was suspended in diethyl ether and stirred with 2 M KOH. After isolation of the organic phase, the aqueous solution was extracted again with diethyl ether, until no solid remained. The organic solvent was dried with Na_2SO_4, and the solvent was removed under reduced pressure, to yield the piperidone P^1 (6.2 g, 12.5 mmol, 33 %). ^{1}H NMR (200 MHz, $[D_3]CH_3CN$, 25 °C, TMS, perchlorate): $\delta = 1.0$ (s, 3H; CH_3), 2.6 (m, 6H; CH_3), 2.8–3.4 (m, 12H; CH_2), 4.2 (dd, $^2J(H,H) = 12$ Hz, $^3J(H,H) = 6$ Hz, 2H; CH), 7.2–7.4 ppm (m, 10H; CH_{Ph}); ^{13}C NMR (50 MHz, $[D_3]CH_3CN$, 25 °C, TMS, perchlorate): $\delta = 15.1$ (1C; CH_3), 45.9 (2C; CH_3), 52.9 (2C; C_{Ph}-C-CH_2), 54.7 (2C; N-CH_2), 56.0 (2C; CH), 58.1 (1C; C$_\cdot$), 62.8 (2C; C-CH_2), 126.9 (2C; $CH_{Ph/p}$), 128.0 (4C; $CH_{Ph/o}$), 129.1 (4C; $CH_{Ph/m}$), 136.5 (2C; C_{Ph}), 205.7 ppm (1C; CO); IR (KBr): $\tilde{\nu} = 3419$ (b), 3087 (m), 3059 (m), 3027 (m), 2967 (s), 2963 (s), 2843 (s), 2801 (s), 1717 (s), 1599 (m), 1496 (m), 1452 (s), 1376 (m), 760 (w), 748 cm^{-1} (w); MS (FAB^+) (nibeol): *m*/*z* (%): 392.3 (100) $[P^1+H]^+$; elemental analysis calcd (%) for $C_{25}H_{34}N_3ClO_5$: C 61.03, H 6.97, N 8.54, Cl 7.21; found: C 60.95, H 6.94, N 8.56, Cl 6.99.

1,5-Diphenyl-3-methyl-7-(1,4,6-trimethyl-1,4-diazacycloheptane-6-yl)diazabicyclo[3.3.1]nonane-9-one (L^1): Methylamine (41 %, 230 mg, 3.0 mmol), formaldehyde (536 mg, 6.6 mmol), and glacial acetic acid (0.7 mL) were mixed at 0 °C in MeOH (6 mL). The ice bath was removed and P^1 (1.173 g, 3.0 mmol) was added. The reaction mixture was stirred for 8 h at 65 °C. After complete removal of the solvents, the resulting orange solid was suspended in diethyl ether. 2 M KOH was added and the two phases were stirred until no insoluble solids remained. The organic phase was isolated and the aqueous phase was extracted twice with diethyl ether. The combined organic phases were dried with Na_2SO_4. The solvent was removed under reduced pressure, yielding L^1 as a white foam, which was used without further purification (1.161 g, 2.6 mmol, 87 %). Analytical data were obtained by crystallization from MeOH. ^{1}H NMR (200 MHz, $[D_1]CHCl_3$, 25 °C, TMS): $\delta = 1.1$ (s, 3H; CH_3), 2.2 (m, 6H; N-CH_3), 2.2 (d, $^2J = 13.4$ Hz, 2H; C-N-CH_{2ax}), 2.4 (m, 3H; N-CH_3), 2.5 (m, 4H; CH_2-CH_2), 2.8 (d, $^2J(H,H) = 13.4$ Hz, 2H; C-N-CH_{2eq}), 3.0 (d, $^2J(H,H) = 10.6$ Hz, 2H; CH_{2ax}-N-CH_3/N-CH_{2ax}-C), (d, $^2J(H,H) = 11.0$ Hz, 2H; N-CH_{2ax}-C/CH_{2ax}-N-CH_3), 3.4(d, $^2J(H,H) = 10.6$ Hz, 2H; CH_{2eq}-N-CH_3/N-CH_{2eq}-C), 3.8 (d, $^2J(H,H) = 11.0$ Hz, 2H; N-CH_{2eq}-C/CH_{2eq}-N-CH_3), 7.2 ppm (m, 10H, CH_{Ph}); ^{13}C NMR (50 MHz, $[D_1]CHCl_3$, 25 °C,

TMS): $\delta = 18.9$ (1C; C-CH_3), 46.0 (1C; N-CH_3), 49.2 (2C; CH_3), 55.8 (1C; C-CH_3), 59.2 (2C; C-C_{Ph}), 60.0 (2C; N-CH_2-C), 62.6 (2C; N-CH_2), 66.7 (2C; N-CH_2-C/CH_2-N-CH_3), 67.3 (2C; N-CH_2-C/CH_2-N-CH_3), 126.8 (2C; $CH_{Ph/p}$), 127.3 (4C; $CH_{Ph/o}$), 128.2 (4C; $C_{Ph/m}$), 143.5 (2C; C_{Ph}), 212.1 ppm (1C; CO); IR (KBr): $\tilde{\nu} = 3022$ (m), 2937 (s), 2802 (s), 1733 (s), 1599 (m), 1575 (m), 1495 (m), 1456 (s), 1320 (m), 761 (w), 693 cm^{-1} (w); MS (FAB$^+$) (nibeol): *m*/*z* (%): 447.4 (100) $[L^1+H]^+$; elemental analysis calcd (%) for $C_{28}H_{38}N_4O$: C 75.30, H 8.58, N 12.54; found: C 75.00, H 8.53, N 12.52.

$[Cu^{II}(L^1)(NCCH_3)](BF_4)_2 \cdot CH_3CN$: Under an argon atmosphere and completely dry conditions, $[Cu^I(NCCH_3)_4](BF_4)$ (132 mg, 0.42 mmol) was dissolved in CH_3CN (3 mL) and added to a solution of L^1 (161 mg, 0.36 mmol) in CH_3CN (3 mL). For the oxidation of Cu^I to Cu^{II}, a 5 mM solution of $AgBF_4$ in CH_3CN was added to the reaction mixture (0.5 mL). After being stirred at RT overnight, the precipitated silver was removed by filtration. To the resulting blue solution diethyl ether was allowed to diffuse, yielding blue crystals (101 mg, 0.14 mmol, 39%). IR (KBr): $\tilde{\nu} = 3450$ (b), 3064 (w), 3029 (w), 2977 (m), 2935 (m), 2248 (s), 1742 (s), 1635 (m), 1479 (m), 1450 (m), 1048 (s), 766 (m), 699 cm^{-1} (m); UV/Vis (CH_3CN): λ (ε) = 903 nm (341 $L\,mol^{-1}\,cm^{-1}$); λ_{max} (ε) = 627 nm (684 $L\,mol^{-1}\,cm^{-1}$); MS (ESI$^+$, CH_3CN) (water due to measurement in ESI machine): *m*/*z* (%): 568 (100) $[Cu^{II}(H_3O)(L^1)(NCCH_3)]^+$, 510 (6) $[Cu^{II}(H)(L^1)]^+$, 275 (62) $[Cu^{II}(L^1)(NCCH_3)]^{2+}$, 255 (14) $[Cu^{II}(L^1)]^{2+}$; elemental analysis calcd (%) for $C_{30}H_{41}N_5B_2CuF_8O$: C 50.18, H 5.79, N 10.97; found: C 50.09, H 5.82, N 10.93; EPR (CH_3CN/toluene 1:1, T = 105 K): $g_{||} = 2.21$ ($A_{||} = 70$ G), $g_{\perp} = 2.08$ ($A_{\perp} = 15$ G); CV: $E_{1/2}$ (CH_3CN, T = 25 °C, 100 mV s^{-1}): −377 (Cu^I/Cu^{II}), +1720 mV (Cu^{II}/Cu^{III}).

$[Cu^{II}(L^1)(NCCH_3)](O_3SCF_3)_2 \cdot CH_3CN$: Under an argon atmosphere and completely dry conditions, $[Cu^{II}](O_3SCF_3)_2$ (122 mg, 0.33 mmol) was dissolved in CH_3CN (2 mL) and then added to a solution of L^1 (150 mg, 0.33 mmol) in CH_3CN (3 mL). After being stirred at RT overnight, diethyl ether was added to the resulting blue solution and allowed to diffuse to yield blue crystals (91.3 mg, 0.11 mmol, 33%). MS (ESI$^+$, CH_3CN): *m*/*z* (%): 658 (100) $[Cu^{II}(L^1)(O_3SCF_3)]^+$, 255 (9) $[Cu^{II}(L^1)]^{2+}$; elemental analysis calcd (%) for $C_{32}H_{41}N_5CuF_6O_7S_2$: C 45.25, H 4.87, N 8.25; found: C 45.21, H 4.93, N 8.30.

1-*tert*-Butyl-2(diacetoxyiodo)-3,4,5-trimethylbenzene:[50] 1-*tert*-Butyl-2-iodo-3,4,5-trime-thylbenzene (1.33 g, 4.4 mmol) was dissolved in glacial acetic acid (40 mL) at 40 °C. After 20 min, sodium perborate tetrahydrate (6.82 g, 44.3 mmol) was added slowly under stirring. After 7 h of being stirred at 40 °C, half of the solvent was removed in vacuo, and water (50 mL) was added. The precipitate was collected and washed twice with cyclohexane to yield (6-*tert*-butyl-2,3,4-trimethylphenyl)methylene diacetate (774 mg, 2.6 mmol, 60%) as a white solid. ^{1}H NMR (200 MHz, $[D_1]CHCl_3$, 25 °C, TMS): $\delta = 1.5$ (s, 9H; C-$(CH_3)_3$), 1.9 (s, 6H; OCO-CH_3), 2.3 (s, 3H; $C_{Ph/C3;C4}$ -CH_3), 2.3 (s, 3H; $C_{Ph/C3;C4}$-CH_3), 2.8 (s, 3H; $C_{Ph/C5}$-CH_3), 7.4 ppm (s, 1H; CH_{Ph}).

***N*-Tosylimino(1-*tert*-butyl-3,4,5-trimethylbenzene)iodinane**:[14] *p*-Toluenesulfonamide (416 mg, 2.43 mmol) and KOH (325 mg, 5.79 mmol) were dissolved in MeOH (8 mL) and cooled to 0 °C. Under stirring, 1-*tert*-butyl-2(diacetoxyiodo)-3,4,5-trimethylbenzene (682 mg, 2.32 mmol) was added at 10 °C. After 1 h of being stirred at 0 °C and 3 h at RT, water (8 mL) was added slowly at 0 °C. After one night in the fridge, a light yellow precipitate was isolated by filtration and washed with a small amount MeOH and cyclohexane, to yield *N*-tosylimino(1-*tert*-butyl-3,4,5-trimethylbenzene)iodinane (764 mg, 1.62 mmol, 70%). Elemental analysis calcd (%) for $C_{20}H_{26}NIO_2S$: C 50.96, H 5.56, N 2.97; found: C 50.94, H 5.52, N 2.96.

Aziridination experiments: For the standard conditions used, see also Table 2;[17,19] the catalyst and styrene or *cis*-β-methylstyrene were dissolved in the dry solvent (see Table 2 for the solvents and concentrations used) before PhINTs was added. When the reaction mixture became clear (the corresponding reaction times are given in Table 2), it was passed through a short neutral aluminia column with ethyl acetate as added solvent (25 mL). The solvents were evaporated under reduced pressure. Anthrone (38.8 mg, 2.0 mmol) was added as internal standard to the resulting solid and the yield was determined by ^{1}H NMR spectroscopy[51] in $CDCl_3$.

X-ray crystal structure determination: Crystal data and structure refinement for $[Cu(L^1)(NCCH_3)](BF_4)_2 \cdot CH_3CN$: $C_{32}H_{44}B_2CuF_8N_6O$; M_r = 765.89; T = 296(2) K; triclinic; space group $P\bar{1}$; a = 10.0530(9), b = 11.9894(11), c = 15.4074(14) Å; α = 100.629(2), β = 99.844(2), γ = 93.785(2)°; V = 1789.2(3) Å^3; Z = 2; ρ_{calcd} = 1.422 $Mg\,m^{-3}$; μ = 0.688 mm^{-1}; $F(000)$ = 794; crystal size 0.25 × 0.20 × 0.05 mm^3; θ range for data collection 1.37–25.09°; 29116 reflections collected; 6340 independent reflections (R_{int} = 0.0541); 4175 observed reflections with $I > 2\sigma(I)$; index ranges (independent set): $h = -11$ to 11, $k = -14$ to 14, l = 0 to 18; completeness to θ: 25.09°, 99.7%; max/min transmission factors: 0.7452/0.6765; data/restraints/parameters 6340/19/485; GOF on F^2 = 1.092; $R(F)$ = 0.0524, $wR(F^2)$ = 0.1272 (observed data, $F_o > 4\sigma(F_o)$); $R(F)$ = 0.1016, $wR(F^2)$ = 0.1606 (all data); difference density: root-mean-square/max/min 0.082/0.541/−0.448 e Å^{-3}. Intensity data were collected with a Bruker AXS Smart 1000 CCD diffractometer ($Mo_{K\alpha}$ radiation, graphite monochromator, λ = 0.71073 Å). Data were corrected for air and detector absorption, and Lorentz and polarization effects;[52] absorption by the crystal was treated with a semiempirical multiscan method.[53,54] The structure was solved by the heavy-atom method combined with structure expansion by direct methods applied to difference structure factors[55,56] and refined by full-matrix least squares methods based on F^2 against all unique reflections.[57,58] All non-hydrogen atoms were given anisotropic displacement parameters. Hydrogen atoms were input at calculated positions and refined with a riding model. The tetrafluoroborate anions were found to be disordered. A split atom model was used and/or B–F and F···F distances were restrained to sensible values during refinement. CCDC-725812 contains the supplementary crystallographic data for this paper. These data can be obtained free of charge from The Cambridge Crystallographic Data Centre via www.ccdc.cam.ac.uk/data_request/cif.

Computational details: DFT calculations were performed by using Jaguar 6.5.[59] Two different basis sets were used, the LACVP basis set BS1[60–63] and the LACV3P**++ basis set BS2.[60–63] Full structural optimizations were carried out with BS1, and BS2 was then used for single-point calculations. For the location of transition states, either the usual transition-state search with a starting geometry obtained with BS1 and B3LYP[64,65] or the synchronous transit-guided quasi-Newton (STQN) method or a combination of both were used. Frequency calculations were performed on all optimized structures to verify their nature and to obtain zero-point corrections to the energies. Unless otherwise stated, all DFT energies and spin densities quoted in this manuscript are derived from B3LYP/LACV3P**++ (BS2) calculations, with solvation (acetonitrile), zero-point, and entropy corrections included.

Acknowledgements

Generous financial support by the German Science Foundation (DFG) is gratefully acknowledged.

[1] D. Tanner, *Angew. Chem.* **1994**, *106*, 625–646; *Angew. Chem. Int. Ed. Engl.* **1994**, *33*, 599–619.
[2] H. C. Kolb, M. G. Finn, K. B. Sharpless, *Angew. Chem.* **2001**, *113*, 2056–2075; *Angew. Chem. Int. Ed.* **2001**, *40*, 2004–2021.
[3] R. S. Coleman, J.-S. Kong, *J. Am. Chem. Soc.* **1998**, *120*, 3538.
[4] J. B. Sweeney, *Chem. Soc. Rev.* **2002**, *31*, 247.
[5] D. A. Evans, M. M. Faul, M. T. Bilodeau, *J. Org. Chem.* **1991**, *56*, 6744.
[6] Z. Lu, W. Zhang, W. D. Wulff, *J. Am. Chem. Soc.* **1994**, *116*, 2742.
[7] P. Müller, C. Fruit, *Chem. Rev.* **2003**, *103*, 2905.
[8] D. A. Evans, M. M. Faul, M. T. Bilodeau, *J. Am. Chem. Soc.* **1994**, *116*, 2742.
[9] H. C. Kolb, M. G. Finn, K. B. Sharpless, *Angew. Chem.* **2001**, *113*, 2056; *Angew. Chem. Int. Ed.* **2001**, *40*, 2004.
[10] A. Yudin in *Aziridines and Epoxides in Organic Synthesis* Wiley-VCH, Weinheim, **2006**, p. 492.
[11] P. A. S. Lowden in *Aziridines and Epoxides in Organic Synthesis* Wiley-VCH, Weinheim, **2006**, p. 399.

[12] S.-M. Au, J. S. Huang, W.-Y. Yu, W.-H. Fung, C.-M. Che, *J. Am. Chem. Soc.* **1999**, *121*, 9120.
[13] J.-L. Liang, J.-S. Huang, X.-Q. Yu, N. Zhu, C.-M. Che, *Chem. Eur. J.* **2002**, *8*, 1563.
[14] Y. Yamada, T. Yamamoto, M. Okawara, *Chem. Lett.* **1975**, 361.
[15] T. P. Albone, P. S. Aujnla, P. C. Taylor, S. Challenger, A. M. Derrick, *J. Org. Chem.* **1998**, *63*, 9569.
[16] Z. Li, R. W. Quan, E. N. Jacobsen, *J. Am. Chem. Soc.* **1995**, *117*, 5889.
[17] J. A. Halfen, J. K. Hallman, J. A. Schultz, J. P. Emerson, *Organometallics* **1999**, *18*, 5435.
[18] F. Mohr, S. A. Binfield, J. C. Fettinger, A. N. Vedernikow, *J. Org. Chem.* **2005**, *70*, 4833.
[19] P. Comba, C. Lang, C. Lopez de Laorden, A. Muruganantham, G. Rajaraman, H. Wadepohl, M. Zajaczkowski, *Chem. Eur. J.* **2008**, *14*, 5313.
[20] P. Brandt, M. J. Södergren, P. G. Andersson, P.-O. Norrby, *J. Am. Chem. Soc.* **2000**, *122*, 8013.
[21] P. Comba, B. Nuber, A. Ramlow, *J. Chem. Soc. Dalton Trans.* **1997**, 347.
[22] H. Börzel, P. Comba, C. Katsichtis, W. Kiefer, A. Lienke, V. Nagel, H. Pritzkow, *Chem. Eur. J.* **1999**, *5*, 1716.
[23] H. Börzel, P. Comba, K. S. Hagen, C. Katsichtis, H. Pritzkow, *Chem. Eur. J.* **2000**, *6*, 914.
[24] H. Börzel, P. Comba, H. Pritzkow, *J. Chem. Soc. Chem. Commun.* **2001**, 97.
[25] H. Börzel, P. Comba, K. S. Hagen, M. Kerscher, H. Pritzkow, M. Schatz, S. Schindler, O. Walter, *Inorg. Chem.* **2002**, *41*, 5440.
[26] P. Comba, C. Lopez de Laorden, H. Pritzkow, *Helv. Chim. Acta* **2005**, *88*, 647.
[27] K. Born, P. Comba, A. Daubinet, A. Fuchs, H. Wadepohl, *J. Biol. Inorg. Chem.* **2006**, *12*, 36.
[28] M. Atanasov, C. Busche, P. Comba, F. El Hallak, B. Martin, G. Rajaraman, J. van Slageren, H. Wadepohl, *Inorg. Chem.* **2008**, *47*, 8112.
[29] P. Comba, M. Merz, H. Pritzkow, *Eur. J. Inorg. Chem.* **2003**, 1711.
[30] P. Comba, M. Kerscher, W. Schiek, *Prog. Inorg. Chem.* **2007**, *55*, 613.
[31] P. Comba, A. Lienke, *Inorg. Chem.* **2001**, *40*, 5206.
[32] P. Comba, M. Kerscher, M. Merz, V. Müller, H. Pritzkow, R. Remenyi, W. Schiek, Y. Xiong, *Chem. Eur. J.* **2002**, *8*, 5750.
[33] P. Comba, A. Hauser, M. Kerscher, H. Pritzkow, *Angew. Chem.* **2003**, *115*, 4675; *Angew. Chem. Int. Ed.* **2003**, *42*, 4536.
[34] P. Comba, M. Kerscher, G. A. Lawrance, B. Martin, H. Wadepohl, S. Wunderlich, *Angew. Chem.* **2008**, *120*, 4818; *Angew. Chem. Int. Ed.* **2008**, *47*, 4740.
[35] A. Bentz, P. Comba, R. J. Deeth, M. Kerscher, H. Pritzkow, B. Seibold, H. Wadepohl, *Inorg. Chem.* **2008**, *47*, 9518.
[36] M. R. Bukowski, P. Comba, C. Limberg, M. Merz, L. Que, Jr., T. Wistuba, *Angew. Chem.* **2004**, *116*, 1303; *Angew. Chem. Int. Ed.* **2004**, *43*, 1283.
[37] M. R. Bukowski, P. Comba, A. Lienke, C. Limberg, C. Lopez de Laorden, R. Mas-Balleste, M. Merz, L. Que, Jr., *Angew. Chem.* **2006**, *118*, 3524; *Angew. Chem. Int. Ed.* **2006**, *45*, 3446.
[38] J. Bautz, M. Bukowski, M. Kerscher, A. Stubna, P. Comba, A. Lienke, E. Münck, L. Que, Jr., *Angew. Chem.* **2006**, *118*, 5810; *Angew. Chem. Int. Ed.* **2006**, *45*, 5681; *Angew. Chem.* **118**, 5810.
[39] J. Bautz, P. Comba, C. Lopez de Laorden, M. Menzel, G. Rajaraman, *Angew. Chem.* **2007**, *119*, 8213; *Angew. Chem. Int. Ed.* **2007**, *46*, 8067.
[40] P. Comba, M. Maurer, P. Vadivelu, *J. Phys. Chem. A* **2008**, *112*, 13028.
[41] A. C. M. Appel, R. Hage, S. W. Russell, D. Tetard, Unilever, WO A 0185717, **2000**; [*Chem. Abstr.* **2001**, *135*, 359431].
[42] R. A. Peralta, A. Neves, A. J. Borloluzzi, A. Casellato, A. dos Anjos, A. Greatti, F. R. Xavier, B. Szpoganicz, *Inorg. Chem.* **2005**, *44*, 7690.
[43] R. Barbucci, M. J. M. Campell, *Inorg. Chim. Acta* **1975**, *15*, L15.
[44] K. M. Gillespie, C. J. Sanders, P. O'Shaughnessy, I. Westmoreland, C. P. Thickitt, P. Scott, *J. Org. Chem.* **2002**, *67*, 3450.
[45] M. M. Diaz-Requejo, P. J. Perez, M. Brookhart, J. L. Templeton, *Organometallics* **1997**, *16*, 4399.
[46] K. M. Gillespie, E. J. Crust, R. J. Deeth, P. Scott, *J. Chem. Soc. Chem. Commun.* **2001**, 785.
[47] D. Wang, G. R. Hanson, *J. Magn. Reson. Ser. A* **1995**, *117*, 209.
[48] D. Wang, G. R. Hanson, *Appl. Magn. Reson.* **1996**, *11*, 401.
[49] "Bispidonliganden und ihre Metallkomplexe": P. Comba, C. Haaf, M. Kerscher, A. Lienke, PCT/EP 2008/004506, **2008**.
[50] A. McKillop, D. Kemp, *Tetrahedron* **1989**, *45*, 3299.
[51] S. Gandhi, A. Bisai, B. A. B. Prasad, V. K. Singh, *J. Org. Chem.* **2007**, *72*, 2133.
[52] SAINT, area detector control and integration software, Bruker AXS, Madison, **2007**.
[53] R. H. Blessing, *Acta Crystallogr. Sect. A* **1995**, *51*, 33.
[54] SADABS-2004–2008, G. M. Sheldrick, Bruker AXS, Madison, **2004–2008**.
[55] P. T. Beurskens in *Crystallographic Computing 3* (Eds.: G. M. Sheldrick, C. Krüger, R. Goddard), Clarendon Press, Oxford, **1985**, p. 216.
[56] P. T. Beurskens, G. Beurskens, R. de Gelder, J. M. M. Smits, S. Garcia-Granda, R. O. Gould *DIRDIF-2008*, Radboud University Nijmegen, The Netherlands, **2008**.
[57] SHELXL-97, G. M. Sheldrick, University of Göttingen, Göttingen, **1997**.
[58] G. M. Sheldrick, *Acta Crystallogr. Sect. A* **2008**, *64*.
[59] JAGUAR 5.5, Schrödinger LLC, New York, **2005**.
[60] T. H. Dunning, Jr., P. J. Hay in *Modern Theoretical Chemistry, Vol. 3* (Ed.: H. F. Schäfer III), Plenum Press, New York, **1976**, p. 1.
[61] P. J. Hay, W. R. Wadt, *J. Chem. Phys.* **1985**, *82*, 270.
[62] R. Ditchfield, W. J. Hehre, J. A. Pople, *J. Chem. Phys.* **1971**, *54*, 724.
[63] V. A. Rassolov, M. A. Ratner, J. A. Pople, P. C. Redfern, L. A. Curtiss, *J. Comput. Chem.* **2001**, *22*, 976.
[64] C. Lee, W. Yang, R. G. Parr, *Phys. Rev. B* **1988**, *37*, 785.
[65] A. D. Becke, *J. Chem. Phys.* **1993**, *98*, 5648.

Received: December 19, 2008
Revised: July 3, 2009
Published online: September 11, 2009

